

Dalton Transactions

An international journal of inorganic chemistry

Accepted Manuscript

This article can be cited before page numbers have been issued, to do this please use: J. Beitzberger, H. Meyer, M. Martin, M. Scheele, M. Ströbele and P. Schmidt, *Dalton Trans.*, 2025, DOI: 10.1039/D5DT00174A.



This is an Accepted Manuscript, which has been through the Royal Society of Chemistry peer review process and has been accepted for publication.

Accepted Manuscripts are published online shortly after acceptance, before technical editing, formatting and proof reading. Using this free service, authors can make their results available to the community, in citable form, before we publish the edited article. We will replace this Accepted Manuscript with the edited and formatted Advance Article as soon as it is available.

You can find more information about Accepted Manuscripts in the [Information for Authors](#).

Please note that technical editing may introduce minor changes to the text and/or graphics, which may alter content. The journal's standard [Terms & Conditions](#) and the [Ethical guidelines](#) still apply. In no event shall the Royal Society of Chemistry be held responsible for any errors or omissions in this Accepted Manuscript or any consequences arising from the use of any information it contains.

ARTICLE

The Family of tetranuclear Nb₄OI_{12-x} Clusters (x = 0, 1, 2): From the molecular Nb₄OI₁₂ cluster to extended chains and layersJan Beitzberger,^a Mario Martin,^b Marcus Scheele,^b Patrick Schmidt,^a Markus Ströbele^a and H.-Jürgen Meyer^{*a}Received 00th January 20xx,
Accepted 00th January 20xx

DOI: 10.1039/x0xx00000x

Abstract. Unconventional reduction reactions in the Nb-O-I system have produced a number of niobium oxyiodides containing the oxygen-centered [Nb₄O] cluster. Crystalline Nb₄OI₁₂ and two modifications of Nb₄OI₁₁ were structurally characterized by means of single-crystal X-ray diffraction studies. The new compounds can be classified as members of the Nb₄OI_{12-x} family, together with the already known Nb₄OI₁₀. Nb₄OI₁₂ is represented by a molecular structure, in which the two modifications of Nb₄OI₁₁ are forming structures with iodido-bridged strings, that can be assigned to represent one-dimensional structures. Measurements of b-Nb₄OI₁₁ single crystals reveal semiconducting behaviour, with an electrical conductivity in the order of 10⁻³ S/m at 300 K and an electrical band gap estimated with 0.4 eV. The presence of varying numbers of cluster electrons in the given compounds is discussed in the light of second-order Jahn-Teller distortion.

Introduction

Metal clusters display a broad variety in structural arrangements and oxidation states. A large number of transition metal (*M*) halide (*X*) clusters have been reported with the octahedral [M₆] cluster core, being represented with [M₆X₁₂]- and [M₆X₈]-type architectures.^[1] The [M₆X₁₂]-type constitutes an octahedral M₆ cluster with twelve *X* atoms capping all edges of the M₆ core and is typically obtained for combinations of larger *M* and smaller *X* atoms. The [M₆X₈] cluster constitutes an octahedral cluster with eight face-capping ligands of the M₆ cluster and is typically obtained for combinations of smaller *M* and larger *X* atoms. The well-known niobium cluster compounds Nb₆Cl₁₄ and Nb₆I₁₁ are good examples of these two architectures, of which the latter can be described as (Nb₆I₈)I^a_{6/2} (*i* = innen or inner; *a* = außen or outer), emphasizing the presence of an [M₆X₈] cluster and a connectivity pattern in which six outer iodide ligands are shared between two clusters.^[2, 3]

The connectivity between adjacent cluster cores and the number of cluster electrons being present has an important impact on the electronic properties of cluster compounds. A connectivity, where inner ligands simultaneously act as outer ones (*i*-*a* and *a*-*i* connectivity), is obtained in Chevrel phases like PbMo₆S₈, which is showing superconducting properties as a

result of metal-to-metal interactions between adjacent clusters.^[4]

A successive dimensional reduction of cluster connectivities is exemplified when going from Nb₆I₁₁ [(Nb₆I₈)I^a_{6/2}] having six shared outer ligands in three dimensions, along to W₆I₁₂ [(W₆I₈)I^a₂I^a_{4/2}] having four bridging apical ligands, creating layers, and finally to BiW₆Cl₁₅ [BiCl₂(W₆Cl₈)Cl^a₃Cl^a_{2/2}] with two bridging apical ligands, creating a linear arrangement of clusters.^[3, 5] Isolated clusters like W₆Cl₁₈ ((W₆Cl₈)Cl^a₆) are held together by van der Waals forces.^[6]

Metal-rich niobium iodides involve the compounds Nb₆I₁₁, Nb₃I₈, NbI₃, and NbI₄.^[3, 7] A promising approach for the expansion of this chemistry is the introduction of another anion to create a heteroanionic metal cluster compound. An early outcome of this approach was the insertion of an interstitial atom (*Z*) into the octahedral [M₆X₁₂]-type cluster core to yield [M₆ZX₁₂], mostly evident with the electron-poorer d-metals (*M* = Zr, Hf).^[8] The formation of an interstitially stabilized cluster is uncommon for [M₆X₈]-type clusters, obviously due to an unfavorable short distance between the interstitial and the face-capping anion, causing repulsion. An exception is Nb₆I₁₁ which can incorporate a hydrogen atom to form the interstitially stabilized compound Nb₆HI₁₁.^[9]

Generally, heteroanionic clusters can also be envisioned to constitute anion replacements in given architectures to induce a modified structure or connectivity pattern of clusters, as exemplified for Nb₆I₉S (derived from Nb₆I₁₁), Nb₃X₇S (*X* = Cl, Br, I) and ANb₃Br₇S with *A* = Rb, Cs (derived from Nb₃X₈).^[10]

The employment of oxide as a heteroanion unavoidably leads to the formation of oxyhalides NbOI₂, NbOI₃ and NbO₂I.^[11] However, it has been demonstrated that new oxyiodide cluster compounds can be obtained under certain conditions. A most recent example of a new oxyiodide cluster is Nb₄OI₁₀, which has

^a J. Beitzberger, P. Schmidt, Dr. M. Ströbele, Prof. Dr. H.-J. Meyer
Section for Solid State and Theoretical Inorganic Chemistry
Institute of Inorganic Chemistry

Auf der Morgenstelle 18, 72076 Tübingen, Germany
E-mail: juergen.meyer@uni-tuebingen.de Address here.

^b M. Martin, Prof. Dr. M. Scheele
Institute of Physical and Theoretical Chemistry
Auf der Morgenstelle 18, 72076 Tübingen, Germany



been characterized as a small band-gap semiconductor showing photoresponse.^[12] Its crystal structure can be easily derived from that of Nb₆I₁₁ by cutting-off two (NbI^{a-a}_{1/2})-groups of (Nb₆I₈)I^{a-a}_{6/2}. The resulting planar [(Nb₄OI₈)I^{a-a}_{4/2}] cluster is allowing the presence of a surplus oxygen atom in the cluster center. The relaxation of inner iodide ligands in this structure is avoiding strong interanionic O–I^a repulsions that would likely inhibit an oxygen centering in Nb₆I₁₁.

The preparation of niobium oxyiodide cluster compounds requires subtle control of reaction conditions and can otherwise lead to the crystallization of the thermodynamic more stable known niobium oxyiodides. Such conditions involve a highly dynamic system including elusive phases whose equilibria depend on the temperature and on local concentrations, as has been previously demonstrated with the newly discovered compound W₂O₃I₄ in the W-O-I system.^[13] By varying the synthetic conditions, we herein describe the crystal structures of three tetranuclear niobium cluster compounds that we have characterized in the Nb-O-I system. The previously reported Nb₄OI₁₀ and the herein described compounds are represented by a [Nb₄O] cluster core that is interconnected in different ways following a dimensional reduction from layers (Nb₄OI₁₀) over strings (Nb₄OI₁₁) to isolated molecules (Nb₄OI₁₂).

Results and Discussion

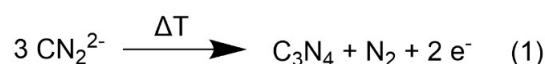
Synthesis and Crystal Structure

Recently, we have described the new cluster compound Nb₄OI₁₀ whose structure is based on a rectangular [Nb₄O] core that is interconnected into layers by iodide ligands.^[12] The crystal structure features a two-dimensional van der Waals material representing a small band gap semiconductor.

Slight variations of the synthesis conditions relative to those

given for Nb₄OI₁₀ revealed the existence of a number of related compounds to exist in the Nb-O-I system. These compounds are generated by changing the concentrations of reaction partners and by subtle variations of the temperature program of reactions. For a general understanding of this type of reaction we have to consider the chemical changes that occur on heating solid reactants in a heterogeneous solid-state reaction with the involvement of solid and gaseous phases. This has been already exemplified by the formation of niobium oxyiodides (NbOI₂, NbOI₃ and NbO₂I) that were described previously.^[11] For the preparation of reduced compounds in the Nb-O-I system, we are avoiding the classical pathway of a metallothermic reduction. Instead, we are exploring unconventional reduction agents with the employment of the carbodiimide ion, (N=C=N)²⁻.

At elevated temperatures, carbodiimides have the tendency to decompose and to act as reducing agents. In this process, metal ions can be reduced, some even to form the metal state.^[14] The decomposition product of carbodiimide in such a reaction is not fully evidenced, as products appear X-ray amorphous. However, infrared spectra indicate the formation of C₃N₄ (Figure S1 and S2).^[15] A corresponding reduction mechanism could follow reaction (1).



All three compounds reported in this work crystallize as black, block-like crystals (Figure 1). They were investigated by X-ray powder and single-crystal diffraction, providing X-ray intensity data for subsequent crystal structure determinations. The crystallographic data and refinement parameters of all tetranuclear cluster compounds are summarized in Table 1.

Syntheses of the new compounds are performed in

Table 1. Crystal data and structure refinement parameters of Nb₄OI_{12-x} compounds.

	Nb ₄ OI ₁₂	a-Nb ₄ OI ₁₁	b-Nb ₄ OI ₁₁	Nb ₄ OI ₁₀ ^[12]
CCDC No.	2366237	2391069	2408695	2225618
Space group	<i>Pmc</i> 2 ₁	<i>C</i> 2/ <i>m</i>	<i>P</i> $\bar{1}$	<i>P</i> 2 ₁ / <i>n</i>
Temperature (K)	270	220	150	150
Unit cell dimensions	<i>a</i> = 37.9189(8) Å <i>b</i> = 17.8026(4) Å <i>c</i> = 7.3403(2) Å	<i>a</i> = 15.4442(3) Å <i>b</i> = 13.0449(2) Å <i>c</i> = 11.9078(2) Å	<i>a</i> = 10.1217(2) Å <i>b</i> = 13.9844(3) Å <i>c</i> = 16.3913(3) Å	<i>a</i> = 10.0435(1) Å <i>b</i> = 10.6595(1) Å <i>c</i> = 10.0594(1) Å
	$\alpha = 90^\circ$ $\beta = 90^\circ$ $\gamma = 90^\circ$	$\alpha = 90^\circ$ $\beta = 105.698(2)^\circ$ $\gamma = 90^\circ$	$\alpha = 88.968(2)^\circ$ $\beta = 89.093(2)^\circ$ $\gamma = 85.329(2)^\circ$	$\alpha = 90^\circ$ $\beta = 94.193(1)^\circ$ $\gamma = 90^\circ$
Volume (Å ³)	4955.1(2)	2309.56(7)	2311.80(8)	1074.06(2)
Z	8	4	2	2
Wavelength (Å)	0.71073	0.71073	0.71073	0.71073
μ (mm ⁻¹)	16.744	16.624	16.607	16.433
2 θ range for data collection	4.576 to 50.700	4.154 to 57.396	7.186 to 76.742	5.532 to 72.638
Total number of reflections	53804	44103	17704	80092
Independent reflections	9037	3115	17704	5209
Refined parameters	418	91	290	71
<i>R</i> _{int}	0.0351	0.0189	0.020	0.0354
<i>R</i> ₁	0.0517	0.0150	0.0185	0.0117
<i>wR</i> ₂	0.1414	0.0314	0.0581	0.0282
Goodness-of-fit on <i>F</i> ²	1.086	1.430	1.037	1.093



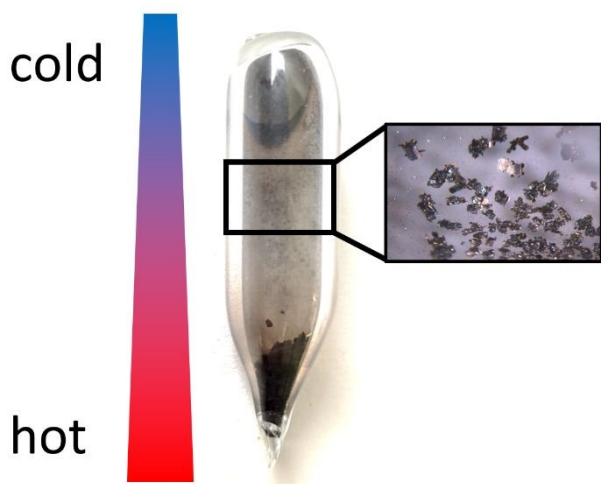


Figure 1. A typical ampoule after the reaction is performed. The temperature gradient during the reaction is illustrated through the bar on the left side (red: hot region, blue cold region). The inset shows the reaction product $b\text{-Nb}_4\text{OI}_{11}$ (see also Figure S4).

evacuated/fused silica tubes at temperatures up to 500 °C. $\text{Nb}_4\text{OI}_{12}$ and $b\text{-Nb}_4\text{OI}_{11}$ were prepared from $\text{NbI}_4\text{:Li}_2(\text{CN}_2)\text{:Li}_2\text{O}$ mixtures with 4:1:1 and 4:1.5:1 molar proportions, respectively. $a\text{-Nb}_4\text{OI}_{11}$ was synthesized by a reaction mixture of $\text{NbI}_4\text{:K}_2\text{CN}_2\text{:Cu}_2\text{O}$ in 4:1.5:1 molar ratio (see Experimental section for more details).

The $\text{Nb}_4\text{OI}_{12-x}$ system includes four structures with sum formulae $\text{Nb}_4\text{OI}_{12}$, $\text{Nb}_4\text{OI}_{11}$, and $\text{Nb}_4\text{OI}_{10}$. $\text{Nb}_4\text{OI}_{11}$ appears with two modifications, denoted as “a” and “b”.

The parent compound $\text{Nb}_4\text{OI}_{12}$ features a molecular structure based on the rectangular $[\text{Nb}_4\text{O}]$ cluster core with eight (μ_2 -) capping and four terminal iodide atoms, shown in Figure 2. The unit cell contains eight molecules that interact through van der Waals bonding. The crystal structure measurement was performed near room temperature because low-temperature measurements revealed incoherent scattering patterns, which could be likely indicative for the appearance of a phase-transition.

Three distinct $\text{Nb}_4\text{OI}_{12}$ molecules are present in the crystal structure. Each of them exhibits a (nearly) rectangular cluster core with six electrons being available for Nb–Nb bonding. The bond lengths of the cluster cores hold a small variability (Figure 2). The short and the long interatomic distances of the cluster are in the range of 2.793(3)–2.807(3) Å and 3.029(7)–3.051(3) Å, suggesting more electron density in each shorter Nb–Nb contact. Regarding the crystal structure, the $\text{Nb}_4\text{OI}_{12}$ molecules are arranged in layers along the ac - and bc -planes (Figure 3). When looking along the b axis (Figure 3, right), the stacking of the molecules in the a direction could be explained as an ABCB sequence, although there is no closest packing of the molecules. The molecules are just arranging to each other in three different bc -planes (denoted in Figure 3 as A, B and C) to reduce repulsion.

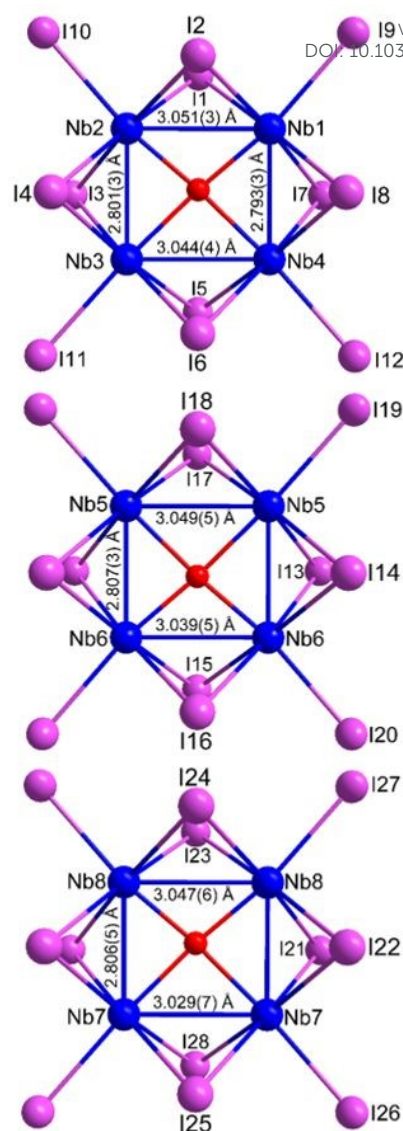


Figure 2. Three distinct $\text{Nb}_4\text{OI}_{12}$ molecules with atom labels and Nb–Nb distances given.

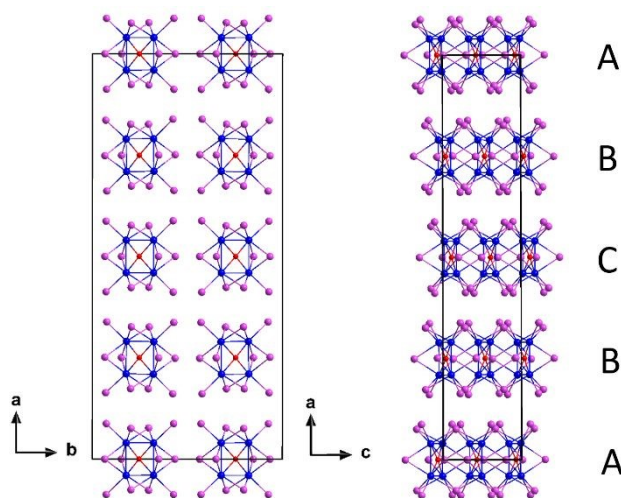


Figure 3. Section of the crystal structure of $\text{Nb}_4\text{OI}_{12}$, looking along the c - and b -axis. Niobium atoms are coloured in blue, iodine in pink, and oxygen in red.



When departing from the molecular $\text{Nb}_4\text{OI}_{12}$ structure, the crystal structure of $\text{Nb}_4\text{OI}_{11}$ contains one iodide atom less and appears with two modifications. We denote these modifications with "a" and "b" because no conversion from one into the other structure could be discovered experimentally. The structure of $a\text{-Nb}_4\text{OI}_{11}$ is represented by a string-like connectivity of $(\text{Nb}_4\text{OI}_8)_{1/2}$ cluster chains, in which each of the two distinct clusters is iodine bridged in a trans connection to the next cluster (Figure 4). The $[\text{Nb}_4\text{O}]$ cluster cores in this structure are as well in a rectangular shape, having two short (2.7368(6)-2.7584(7) Å) and two long (3.0375(6)-3.0423(6) Å) Nb–Nb distances.

The presence of Nb2 atoms over all equivalent (8j) positions would create a layered structure with $[\text{Nb}_4\text{O}]$ - and $[\text{Nb}_6\text{O}]$ -cluster cores, shown in Figure 5. However, the Nb2 positions (highlighted in light blue) are occupied by only $\frac{1}{2}$ resulting in a string connectivity. In fact, this picture (Figure 5) represents a superposition of the alternating layers in the structure. The crystal structure of $a\text{-Nb}_4\text{OI}_{11}$ is characterized by two alternating layers of $(\text{Nb}_4\text{OI}_8)_{1/2}$ that are stacked on top of each other along the [100] direction. The cluster strings within the alternating layers in the structure, each of them shown in Figure 6, are running in two different directions ([011] and [01-1]). This arrangement affords an alternating occupation of Nb2 positions in each layer. The adhesion between adjacent strings and layers in the structure can be described as van der Waals type, forming a hexagonal packing of strings.

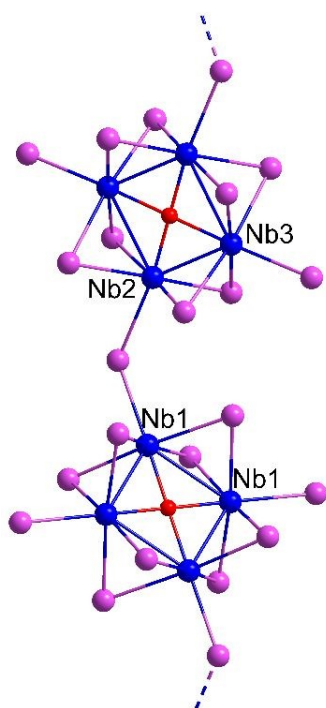


Figure 4. String-like connectivity in the structure of $a\text{-Nb}_4\text{OI}_{11}$.

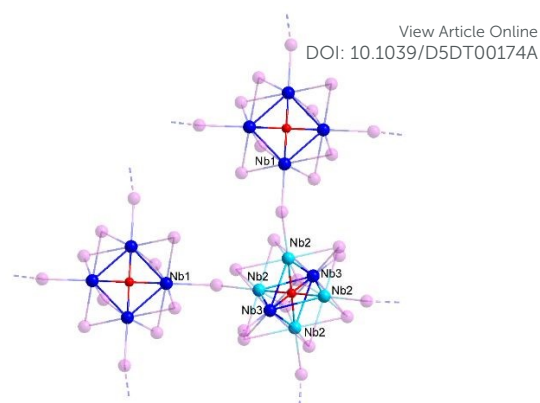


Figure 5. Cluster connectivity in the structure of $a\text{-Nb}_4\text{OI}_{11}$ with the equivalent Nb2 positions coloured in cyan. Due to the half-occupation of Nb2 sites, only one pair of Nb2 atoms is present.

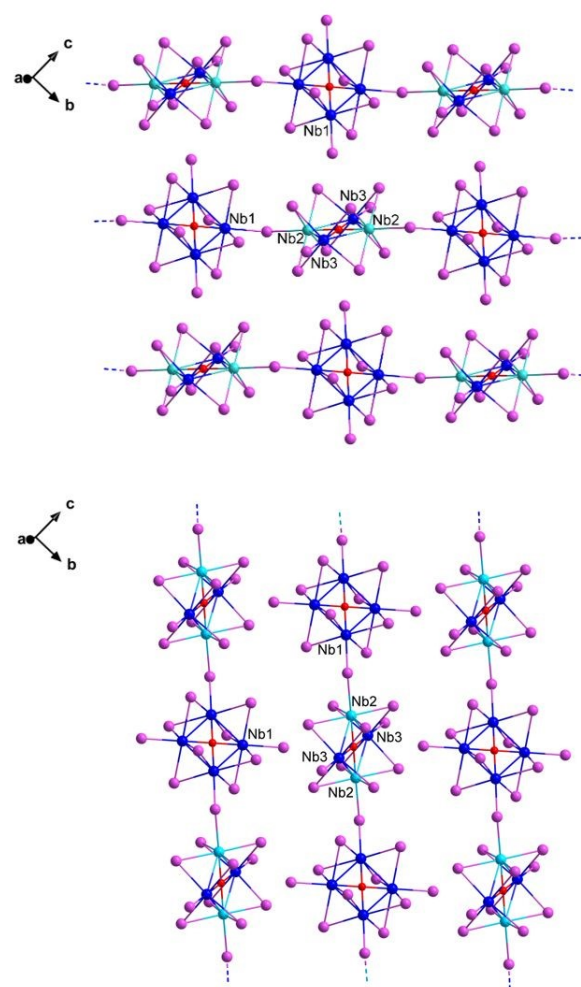


Figure 6. Arrangement of individual cluster layers in the structure, based on string-like connectivities in the structure of $a\text{-Nb}_4\text{OI}_{11}$.

Another modification of $\text{Nb}_4\text{OI}_{11}$ is denoted as $b\text{-Nb}_4\text{OI}_{11}$. The crystal structure of $b\text{-Nb}_4\text{OI}_{11}$ again features a string-like connectivity of two distinct $[\text{Nb}_4\text{O}]$ clusters. However, the connectivity pattern via iodine atoms alternates with a cis and a trans connectivity of $[\text{Nb}_4\text{O}]$ cores. Each trans connected



cluster includes two short and two long Nb–Nb distance within the $[\text{Nb}_4\text{O}]$ core. The same is true for the cis connected cluster. However, the cis connectivity induces a significant distortion to the cluster, specified in Table 2.

The unit cell of the crystal structure of $\text{b-Nb}_4\text{OI}_{11}$ is projected in Figure 7. In contrast to the bidirectional arrangement of cluster strings in the structure of $\text{a-Nb}_4\text{OI}_{11}$, all cluster strings in $\text{b-Nb}_4\text{OI}_{11}$ are running parallel into one direction ($[001]$). A view on the projected ab -plane suggests that the separate strings are held together by van der Waals interactions. The given arrangement of $(\text{Nb}_4\text{OI}_8)_{1/2}(\text{I}_2)_{1/2}$ chains be derived from a hexagonal packing of strings, which is a typical structure pattern observed for one-dimensional structures (Figure 8).

Electrical conductivity of $\text{b-Nb}_4\text{OI}_{11}$

Crystal structures like those of a- and $\text{b-Nb}_4\text{OI}_{11}$ with one-dimensional connectivities may be expected to act as one-dimensional conductors. Hence, the electrical conductivity properties of single crystals of $\text{b-Nb}_4\text{OI}_{11}$ were investigated.

In Figure 9, we display a two-point probe I - U sweep of a typical rod-shaped $\text{b-Nb}_4\text{OI}_{11}$ crystal from which we calculate the electrical conductivity as $\sigma = 4.5 \cdot 10^{-3} \text{ S/m}$ at 300 K. [16, 17]

The temperature-dependent conductivity measurement in Figure 10 indicates an Arrhenius-type, temperature-activated transport, which is typical for semiconducting materials. [12, 17, 18]

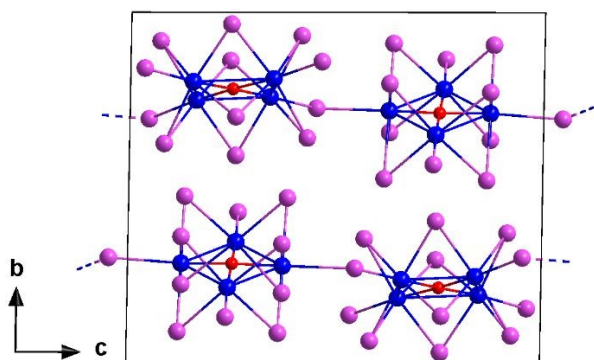


Figure 7. Section of the crystal structure of $\text{b-Nb}_4\text{OI}_{11}$, looking along $[100]$.

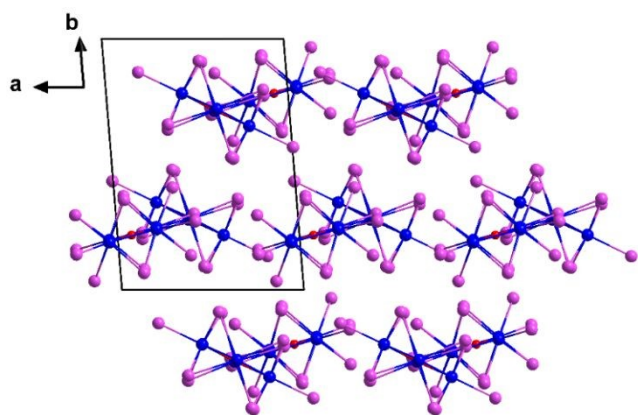


Figure 8. Section of the crystal structure of $\text{b-Nb}_4\text{OI}_{11}$, following the $[001]$ string direction.

From this plot, we obtain an activation energy of $E_a = 0.2 \text{ eV}$. Thus, in a first-order approximation the energy difference of the Fermi level to the conduction band can be gauged as 0.2 eV . Under the assumption of an intrinsic position of the Fermi level, this would suggest an electrical band gap on the order of 0.4 eV . The photoresponse at 300 K of $\text{b-Nb}_4\text{OI}_{11}$ toward optical excitation with a 779 nm laser in continuous wave mode is shown in Figure 11. An initial fast photocurrent of $\sim 65 \text{ nA}$ is followed by a slower, second component under continuous excitation. We attribute this slow component to thermal excitation by heating the crystal with the laser. At lower temperature, the photocurrent decreases substantially, e.g. to 12.6 pA at 160 K.

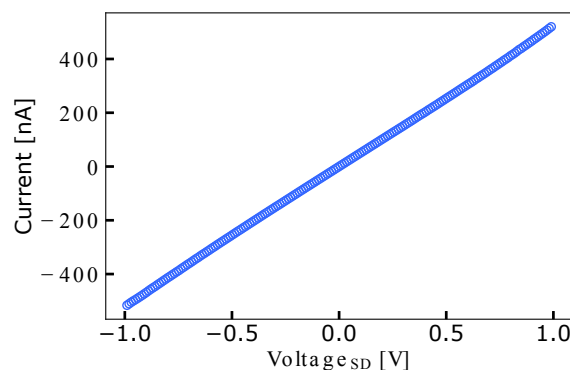


Figure 9. I - U sweep in the dark of a $\text{b-Nb}_4\text{OI}_{11}$ crystal at 300 K.

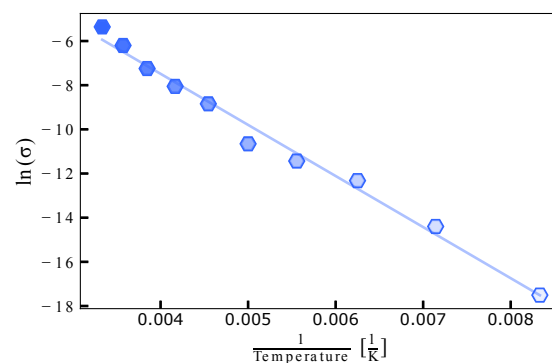


Figure 10. Arrhenius plot of the electrical conductivity of $\text{b-Nb}_4\text{OI}_{11}$, with 20 K temperature steps between 120–300 K. The blue line represents a linear Arrhenius fit to the data.

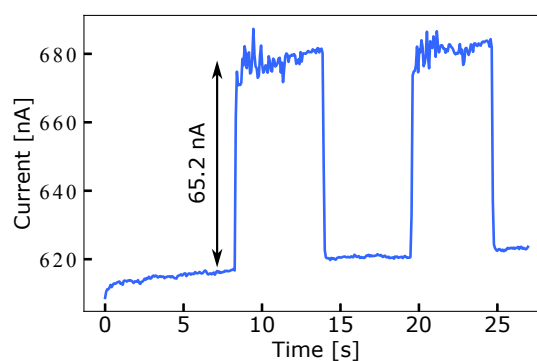


Figure 11. Photoresponse of a $\text{b-Nb}_4\text{OI}_{11}$ crystal at 300 K toward a 779 nm laser illumination with 1 V bias applied.



Electronic properties of Nb₄OI_{12-x} compounds

One member of the Nb₄OI_{12-x} family was already described before as Nb₄OI₁₀.^[12] Nb₄OI₁₀ appears with black, plate-like crystals with an electronic band gap near 0.4 eV, according to an experimental bandgap determination and band structure calculation. This compound contains (Nb₄OI₈)_{4/2} units that are connected into layers, through four shared apical iodide atoms

(**Figure 12**). The cluster core itself is rectangular with Nb–Nb distances of 2.6232(2) Å and 3.1042(2) Å. This compound was

Table 2. The Nb₄OI_{12-x} family with the respective number of cluster electrons of each compound, interatomic distances with average values ($\bar{\varnothing}$) and distance ranges along the short and long cluster edges, and angles within the [Nb₄O] cluster core.

Distances and angles	Nb ₄ OI ₁₂ 6 cluster-e ⁻	a-Nb ₄ OI ₁₁ 7 cluster-e ⁻	b-Nb ₄ OI ₁₁ (trans) 7 cluster-e ⁻	b-Nb ₄ OI ₁₁ (cis) 7 cluster-e ⁻	Nb ₄ OI ₁₀ ^[12] 8 cluster-e ⁻
short Nb–Nb (Å)	$\bar{\varnothing}$ 2.802 2.793(3)-2.807(3)	$\bar{\varnothing}$ 2.748 2.7368(6)-2.7584(7)	$\bar{\varnothing}$ 2.735 2.7329(8)-2.7369(8)	$\bar{\varnothing}$ 2.729 2.7288(8)-2.7299(8)	2.6232(2)
long Nb–Nb (Å)	$\bar{\varnothing}$ 3.044 3.029(7)-3.051(3)	$\bar{\varnothing}$ 3.040 3.0375(6)-3.0423(6)	$\bar{\varnothing}$ 3.054 3.0423(8)-3.0656(8)	$\bar{\varnothing}$ 3.056 2.9168(7)-3.1950(8)	3.1042(2)
small Nb–Nb–Nb (°)	89.81(9)-89.93(9)	87.47(2)	87.34(2)-87.88(2)	87.01(2)-87.14(2)	89.568(6)
large Nb–Nb–Nb (°)	90.11(8)-90.23(9)	92.53(1)	92.17(2)-92.60(2)	92.87(2)-92.97(2)	90.431(6)

reported with an electrical conductivity of $\sigma \approx 1$ S/m at 300 K. Beside their different connectivities, the cluster compounds of the Nb₄OI_{12-x} family differ not only in their Nb–Nb bond lengths and Nb–Nb–Nb angles, but also by their numbers of cluster electrons, as summarized in **Error! Reference source not found.**^[12]

From Nb₄OI₁₂ to Nb₄OI₁₀ there is a difference of two electrons being available for niobium-to-niobium bonding. All compounds are forming nearly rectangular [Nb₄O] clusters in which the longer edges possess almost the same Nb–Nb distances (see Table 2). For the example of Nb₄OI₁₀ we already discussed the higher stability of a rectangular versus a square cluster core. The resulting symmetry lowering goes along with an increase in hybridization of molecular orbitals through a second-order Jahn-Teller distortion. In other words, the series of compounds are showing higher electron localization within the two shorter edges of [Nb₄O] cluster cores. The rectangular niobium

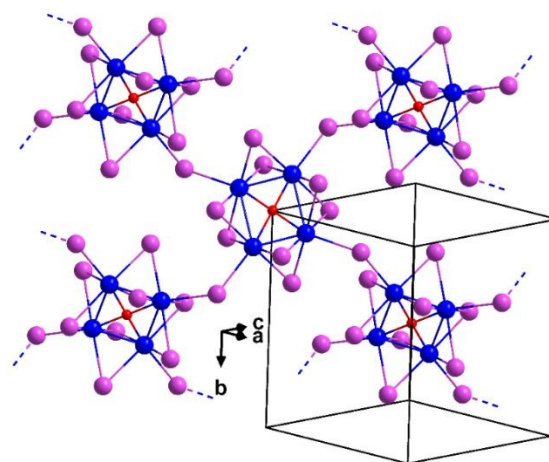


Figure 12. Visualization of the connectivity of Nb₄OI₁₀.^[12]

Table 2. The Nb₄OI_{12-x} family with the respective number of cluster electrons of each compound, interatomic distances with average values ($\bar{\varnothing}$) and distance ranges along the short and long cluster edges, and angles within the [Nb₄O] cluster core.

Distances and angles	Nb ₄ OI ₁₂ 6 cluster-e ⁻	a-Nb ₄ OI ₁₁ 7 cluster-e ⁻	b-Nb ₄ OI ₁₁ (trans) 7 cluster-e ⁻	b-Nb ₄ OI ₁₁ (cis) 7 cluster-e ⁻	Nb ₄ OI ₁₀ ^[12] 8 cluster-e ⁻
short Nb–Nb (Å)	$\bar{\varnothing}$ 2.802 2.793(3)-2.807(3)	$\bar{\varnothing}$ 2.748 2.7368(6)-2.7584(7)	$\bar{\varnothing}$ 2.735 2.7329(8)-2.7369(8)	$\bar{\varnothing}$ 2.729 2.7288(8)-2.7299(8)	2.6232(2)
long Nb–Nb (Å)	$\bar{\varnothing}$ 3.044 3.029(7)-3.051(3)	$\bar{\varnothing}$ 3.040 3.0375(6)-3.0423(6)	$\bar{\varnothing}$ 3.054 3.0423(8)-3.0656(8)	$\bar{\varnothing}$ 3.056 2.9168(7)-3.1950(8)	3.1042(2)
small Nb–Nb–Nb (°)	89.81(9)-89.93(9)	87.47(2)	87.34(2)-87.88(2)	87.01(2)-87.14(2)	89.568(6)
large Nb–Nb–Nb (°)	90.11(8)-90.23(9)	92.53(1)	92.17(2)-92.60(2)	92.87(2)-92.97(2)	90.431(6)

arrangement hosts six electrons for Nb₄OI₁₂, seven electrons for Nb₄OI₁₁, and eight electrons for Nb₄OI₁₀, thereby undergoing a continuous shrinkage of the short Nb–Nb distance, with the values given in Table 2.

If there were less than six electrons for Nb–Nb bonding, the bond lengths should elongate even more. Such a compound is not yet known in the Nb–O–I system. However, the structure of Nb₄OTe₉I₄ contains an oxygen centered Nb₄ cluster core having four cluster electrons for Nb–Nb bonding.^[19] The cluster is distorted into a flattened tetrahedral shape with nearly equal Nb–Nb distances of 3.057(4) Å and 3.050(3) Å. These are quite close to the long distances present in the [Nb₄O] cluster cores presented in this work.



Conclusion

Cluster compounds can show a broad flexibility in their oxidation states. A well-established example is the binary tungsten-iodide system, with more than 20 different structures being reported.^[20] The addition of oxygen leads into the W-O-I system, that is well-known because WO_2I_2 is a prominent compound in chemical vapor transport (CVT) reactions.^[13] The thermal treatment of WO_2I_2 leads to $\text{W}_2\text{O}_3\text{I}_4$ first, and then to WO_2 . All oxides and oxyiodides in this system appear under discrete temperature conditions.

An even broader chemistry is now discovered in the Nb-O-I system for $\text{Nb}_4\text{OI}_{12-x}$ ($x = 0, 1, 2$) compounds, with their rectangular $[\text{Nb}_4\text{O}]$ cluster cores appearing in layers, strings, and in isolated molecules. The distinct connectivity patterns in the crystal structures involve different semiconducting properties.

These compounds could not be prepared in conventional reduction attempts through metallothermic reduction. In contrast, comparably soft reduction conditions were successful, with the carbodiimide ion as reducing agent. Hence, the formation of compounds in the Nb-O-I system involves unconventional reduction reactions in heterogeneous solid-state reactions. The product formation involves subtle equilibrium conditions related to small changes in temperature and local concentrations. These conditions appear fairly complex and are further complicated by other new compounds that exist in the given Nb-O-I system besides the herein described tetranuclear cluster compounds. The discovery of compounds with pentanuclear and heptanuclear niobium clusters in the Nb-O-I system will be reported shortly.

View Article Online
DOI: 10.1039/D5DT00174A



Experimental Section

Materials and methods

Manipulations of starting materials and products were performed in a glovebox under dry argon with moisture and oxygen levels below 1 ppm. Reaction partners were charged into silica tubes ($V \approx 1.5 \text{ cm}^3$). Li_2O (ABCR, 95 %) and Cu_2O (Sigma-Aldrich, 99.99 %) were used as purchased. NbI_4 , $\text{Li}_2(\text{CN}_2)$ and $\text{K}_2(\text{CN}_2)$ were synthesized as described in the literature.^[21] $\text{Nb}_4\text{OI}_{10}$ was synthesized as described before.^[12]

Syntheses

$\text{b-Nb}_4\text{OI}_{11}$ and $\text{Nb}_4\text{OI}_{12}$ were synthesized from NbI_4 , Li_2O and $\text{Li}_2(\text{CN}_2)$. For this purpose, NbI_4 (160.8 mg, 0.268 mmol), Li_2O (2 mg, 0.067 mmol), and $\text{Li}_2(\text{CN}_2)$ (5.4 mg, 0.101 mmol ($\text{b-Nb}_4\text{OI}_{11}$) or 3.6 mg, 0.067 mmol ($\text{Nb}_4\text{OI}_{12}$)) were encapsulated into fused silica ampoules. The ampoules were heated from room temperature to 500 °C with a rate of 0.1 °C/min. The holding time was 24 h before the reactions were allowed to cool to room temperature with a rate of 5 °C/min for $\text{b-Nb}_4\text{OI}_{11}$ and a rate of 10 °C/min for $\text{Nb}_4\text{OI}_{12}$. Block-like crystals of $\text{b-Nb}_4\text{OI}_{11}$ and $\text{Nb}_4\text{OI}_{12}$ were found on the wall of the ampoule, along with some NbOI_2 and NbI_5 at the top of the ampoule. The products were collected mechanically. The compounds are sensitive to moisture. A powder XRD pattern of $\text{b-Nb}_4\text{OI}_{11}$ is shown in Figure S3. Examples of crystal specimens of $\text{b-Nb}_4\text{OI}_{11}$ and $\text{Nb}_4\text{OI}_{12}$ can be seen in Figure S4 and S5.

$\text{a-Nb}_4\text{OI}_{11}$ was synthesized from NbI_4 , Cu_2O and $\text{K}_2(\text{CN}_2)$. For this purpose, NbI_4 (100.7 mg, 0.168 mmol), Cu_2O (6 mg, 0.042 mmol), and $\text{K}_2(\text{CN}_2)$ (7.4 mg, 0.063 mmol) were encapsulated into a fused silica ampoule. The ampoule was heated from room temperature to 500 °C with a rate of 0.1 °C/min. The holding time was 24 h before the reaction was allowed to cool to room temperature with a rate of 5 °C/min. Block-like crystals of $\text{a-Nb}_4\text{OI}_{11}$ were found on the wall of the ampoule, along with some NbOI_2 and NbI_5 at the top of the ampoule. The product was collected mechanically. The compound is sensitive to moisture.

Instrumentation

X-ray diffraction

Black block-shaped single-crystals of $\text{a-Nb}_4\text{OI}_{11}$, $\text{b-Nb}_4\text{OI}_{11}$, and $\text{Nb}_4\text{OI}_{12}$ were mounted on a Rigaku XtaLab Synergy-S X-ray diffractometer using $\text{Mo-K}\alpha$ ($\lambda = 0.71073 \text{ \AA}$) radiation. The single-crystal was kept under N_2 cooling at 270 K for $\text{Nb}_4\text{OI}_{12}$, at 220 K for $\text{a-Nb}_4\text{OI}_{11}$ and at 150 K for $\text{b-Nb}_4\text{OI}_{11}$ during the data collection. Corrections for absorption effects were applied with CrysAlisPro (Rigaku Oxford Diffraction, 2020). The crystal structure was solved by the integrated space group and crystal structure determination routine of ShelXT^[22] and refined by full-matrix least-squares refinement with ShelXL-2019/3^[22] implemented in Olex2.^[23]

Reaction products were investigated by powder X-ray diffraction (PXRD) using a StadiP diffractometer (Stoe, Darmstadt) with $\text{Ge}[111]$ -monochromated $\text{Cu-K}\alpha_1$ radiation and a Mythen1 detector.

Electrical conductivity

Conductivity measurements were performed in a Lake Shore Cryotronics CRX-6.5K probe station with a Keithley 2636B source meter unit. Block-shaped $\text{b-Nb}_4\text{OI}_{11}$ crystals were contacted with silver paste on a silicon substrate with 770 nm oxide layer and transferred into the chamber under protective gas. The conductive silver pads at each end of the crystals were connected to the circuit with tungsten tips. The chamber was kept under vacuum ($<5 \cdot 10^{-5}$ mbar) with 20 K temperature steps between 120 K and 300 K during the measurements. Two-point conductivity measurements were performed by varying the applied source-drain voltage from -1 V to 1 V while detecting the current. For time-resolved photocurrent measurements, using a picosecond pulsed laser driver (Taiko PDL M1, PicoQuant) together with a 779 nm laser head (pulse length <500 ps) the crystals were illuminated at 40 mW laser output power using the continuous wave mode under a constant bias of 1 V.

Conflicts of interest

The authors declare no conflict of interest.

Data availability

The data that support the findings of this study are available from the corresponding author upon reasonable request.

Supporting Information

IR spectra, X-ray diffraction pattern of $\text{b-Nb}_4\text{OI}_{11}$, photographs of crystals.

Acknowledgements

This research was supported by the Deutsche Forschungsgemeinschaft (ME 914-32/1 and SCHE1905/9-1).

References

- [1] L. Pauling, *The Nature of the Chemical Bond and the Structure of Molecules and Crystals: An Introduction to Modern Structural Chemistry*, Cornell University Press, 1960.
- [2] A. Simon, H. Georg Schnering, H. Wöhrle, H. Schäfer, *Zeitschrift für anorganische und allgemeine Chemie* **1965**, 339, 155-170.
- [3] A. Simon, H.-G. Schnering, H. Schäfer, *Zeitschrift für anorganische und allgemeine Chemie* **1967**, 355, 295-310.
- [4] O. Peña, *Physica C: Superconductivity and its Applications* **2015**, 514, 95-112.
- [5] M. Ströbele, H.-J. Meyer, *Zeitschrift für anorganische und allgemeine Chemie* **2009**, 635, 1517-1519; M. Ströbele, H.-J. Meyer, *Inorganic Chemistry* **2017**, 56, 5880-5884.
- [6] R. Siepmann, H. G. V. Schnering, H. Schäfer, *Angewandte Chemie* **1967**, 79, 650-650.



- [7] A. Simon, H. G. Von Schnering, *Journal of the Less Common Metals* **1966**, *11*, 31-46; L. F. Dahl, D. L. Wampler, *Acta Crystallographica* **1962**, *15*, 903-911; P. W. Seabaugh, J. D. Corbett, *Inorganic Chemistry* **1965**, *4*, 176-181.
- [8] R. P. Ziebarth, J. D. Corbett, *Journal of the Less Common Metals* **1988**, *137*, 21-34; R. P. Ziebarth, J. D. Corbett, *Journal of Solid State Chemistry* **1989**, *80*, 56-67; J. Zhang, J. D. Corbett, *Journal of Solid State Chemistry* **1994**, *109*, 265-271; J. Zhang, J. D. Corbett, *Inorganic Chemistry* **1991**, *30*, 431-435; J. D. Smith, J. D. Corbett, *Journal of the American Chemical Society* **1984**, *106*, 4618-4619; R.-Y. Qi, J. D. Corbett, *Inorganic Chemistry* **1994**, *33*, 5727-5732.
- [9] A. Simon, *Zeitschrift für anorganische und allgemeine Chemie* **1967**, *355*, 311-322.
- [10] H.-J. Meyer, J. D. Corbett, *Inorganic Chemistry* **1991**, *30*, 963-967; P. J. Schmidt, G. Thiele, *Acta Crystallographica Section C* **1997**, *53*, 1743-1745; G. V. Khvorykh, A. V. Shevelkov, V. A. Dolgikh, B. A. Popovkin, *Journal of Solid State Chemistry* **1995**, *120*, 311-315; C. M. Pasco, Johns Hopkins University **2021**; F. Grahlow, F. Strauß, M. Scheele, M. Ströbele, A. Carta, S. F. Weber, S. Kroeker, C. P. Romao, H.-J. Meyer, *Physical Chemistry Chemical Physics* **2024**, *26*, 11789-11797; H.-J. Meyer, *Zeitschrift für anorganische und allgemeine Chemie* **1994**, *620*, 863-866.
- [11] J. Rijnsdorp, F. Jellinek, *Journal of the Less Common Metals* **1978**, *61*, 79-82; S. Hartwig, Dissertation, Bayreuth **2003**.
- [12] J. Beitzberger, M. Ströbele, F. Strauß, M. Scheele, C. P. Romao, H.-J. Meyer, *European Journal of Inorganic Chemistry* **2024**.
- [13] M. Löber, M. Ströbele, C. P. Romao, H.-J. Meyer, *Dalton Transactions* **2021**, *50*, 6789-6792.
- [14] K. Gibson, M. Ströbele, B. Blaschkowski, J. Glaser, M. Weissner, R. Srinivasan, H. J. Kolb, H.-J. Meyer, *Zeitschrift für anorganische und allgemeine Chemie* **2003**, *629*, 1863-1870.
- [15] H. Zhao, X. Chen, C. Jia, T. Zhou, X. Qu, J. Jian, Y. Xu, T. Zhou, *Materials Science and Engineering: B* **2005**, *122*, 90-93; H. Li, Y. Jing, X. Ma, T. Liu, L. Yang, B. Liu, S. Yin, Y. Wei, Y. Wang, *RSC advances* **2017**, *7*, 8688-8693.
- [16] F. Fetzer, A. Maier, M. Hodas, O. Geladari, K. Braun, A. J. Meixner, F. Schreiber, A. Schnepf, M. Scheele, *Nat Commun* **2020**, *11*, 6188; D. Meschede, *Gerthsen Physik, Vol. 22*, Springer, **2004**.
- [17] F. Grahlow, F. Strauß, P. Schmidt, J. Valenta, M. Ströbele, M. Scheele, C. P. Romao, H.-J. Meyer, *Inorganic Chemistry* **2024**, *63*, 19717-19727.
- [18] M. M. A. Imran, O. A. Lafi, *Physica B: Condensed Matter* **2013**, *410*, 201-205; A. M. Al-Fa'ouri, O. A. Lafi, H. H. Abu-Safe, M. Abu-Kharma, *Arabian Journal of Chemistry* **2023**, *16*; K. Kiran Kumar, M. Ravi, Y. Pavani, S. Bhavani, A. K. Sharma, V. V. R. Narasimha Rao, *Physica B: Condensed Matter* **2011**, *406*, 1706-1712; A. S. Hassanien, A. A. Akl, *Journal of Non-Crystalline Solids* **2016**, *432*, 471-479.
- [19] W. Tremel, *Journal of the Chemical Society, Chemical Communications* **1992**, 709-710.
- [20] M. Ströbele, H.-J. Meyer, *Dalton Transactions* **2019**, *48*, 1547-1561.
- [21] G. Brauer, *Handbuch der präparativen anorganischen Chemie*, Enke, **1975**; R. Srinivasan, M. Ströbele, H. J. Meyer, *Inorganic Chemistry* **2003**, *42*, 3406-3411; M. Ströbele, E. Bayat, H.-J. Meyer, *Inorganic Chemistry* **2024**, *63*, 16565-16572.
- [22] G. Sheldrick, *Acta Crystallographica Section C* **2015**, *71*, 3-8. [View Article Online](#)
DOI: 10.1039/D5DT00174A
- [23] O. V. Dolomanov, L. J. Bourhis, R. J. Gildea, J. A. K. Howard, H. Puschmann, *Journal of Applied Crystallography* **2009**, *42*, 339-341.



Data availability

View Article Online
DOI: 10.1039/D5DT00174A

Crystallographic data have been deposited at the CCDC under 2366237 ($\text{Nb}_4\text{OI}_{12}$), 2391069 (a- $\text{Nb}_4\text{OI}_{11}$), and 2408695 (b- $\text{Nb}_4\text{OI}_{11}$).

Data are available within the article

The data that support the findings of this study are available on request from the corresponding author, H.-J. Meyer

